



## Adsorption process and mechanism for furfural separation with macroporous resin

Chunmei Jia<sup>a</sup>, Xinying Li<sup>b</sup>, Zhen Liu<sup>a</sup>, Bin Xu<sup>a</sup>, Shun Yao<sup>a</sup>, Hang Song<sup>a,\*</sup>

<sup>a</sup>School of Chemical Engineering, Sichuan University, Chengdu 610065, P.R. China, Tel./Fax: +86 28 8540 5221; emails: [jia\\_227326@163.com](mailto:jia_227326@163.com) (C. Jia), [13541386560@163.com](mailto:13541386560@163.com) (Z. Liu), [jia.227@tom.com](mailto:jia.227@tom.com) (B. Xu), [cusack@scu.edu.cn](mailto:cusack@scu.edu.cn) (S. Yao), [hangsong@scu.edu.cn](mailto:hangsong@scu.edu.cn) (H. Song)

<sup>b</sup>College of Chemistry and Environment Protection Engineering, Southwest University for Nationalities, Chengdu 610041, P.R. China, Tel. +85928015; email: [silverstar8402@163.com](mailto:silverstar8402@163.com) (X. Li)

Received 10 November 2013; Accepted 21 August 2014

---

### ABSTRACT

At present, a high-temperature steam requirement is the main problem in the recovery of furfural. In this work, D141 macroporous resin was selected to separate and enrich furfural from the hydrolysate, and ethanol was selected as the desorption reagent. The adsorption selectivity of furfural and acetic acid made it possible to obtain acetic acid simultaneously. Adsorption kinetics revealed that the rate was rapid and fitted by a pseudo-second-order model. Then the breakthrough curve and optimal operation conditions were systematically investigated. The optimized process of adsorption was a 3 bed volume (BV) solution loaded on the fixed bed of the D141 resin with a velocity of 1 BV/h, then eluted by 1 BV ethanol with a velocity of 1 BV/h. As a result, 96.97% of final recovery yield of furfural was obtained. Compared with the previous studies, the D141 macroporous resin was found to be more favorable for the adsorption of furfural in the hydrolysate.

*Keywords:* Furfural; Adsorption; Desorption; Macroporous resin

---

### 1. Introduction

Furfural is a versatile key derivative produced from pentosan-rich biomass [1]. It can be converted to furfuryl alcohol and subsequently upgraded to levulinic acid or levulinic esters. Alternatively, it can be reformed to furanic biofuels, which drew attention from the utilization of lignocellulosic biomass [2]. In its traditional preparation process, hemicellulose materials were treated with strong acid to convert the hemicellulose fraction into pentose carbohydrates, which were further cyclodehydrated to furfural. Rapid flashing of furfural from the reaction medium was

needed to avoid consecutive degradation. Such flashing was accompanied with the excessive evaporation of water, and thereby, a steam consumption of approximately  $30 \text{ t}_{\text{furfural}}^{-1}$  was required [2]. Furfural was then recovered from the dilute aqueous system by distillation. However, a heterogeneous azeotrope was formed by furfural and water (atmospheric composition 35 wt% or 10 mol% furfural at 97.8°C), which dispersed naturally into the furfural-rich phase and water-rich phase after condensation [3]. The water-rich phase still contains approximately 8 wt% of furfural that was recycled from the azeotropic distillation column for further furfural recovery. As a result of the very diluted aqueous furfural feed and the existence

---

\*Corresponding author.

of the azeotrope, the recovery of furfural consumed a large amount of steam. Thus, new research is urgently needed to improve furfural recovery from the diluted aqueous product [2].

In terms of the higher efficiency of furfural recovery, the use of liquid–liquid extraction was recommended [4–6], and the mixture of solvent and furfural were further separated by steam distillation. Supercritical CO<sub>2</sub> [7], polymer sorbents [8], membrane separation [9,10], biphasic hydrolysis system [11,12], and nitrogen [13] have also been extensively studied to recover furfural from the aqueous phase. Despite all the novel developments described above, the cost and energy needed for furfural production required further improvements [2].

Adsorption is regarded as a practical and energy-efficient method for purification or bulk separation with all kinds of materials, such as biomass products, fine chemicals, or industrial wastes [14]. Despite the numerous studies reported in the literature involving furfural adsorption [8,14–18], the focus was mainly on the recovery of furfural from wastewater. The hydrolyzed product of biomass with higher concentration and byproducts has received little attention.

The aim of the present work is the exploration of the possibility of the adsorptive separation of furfural from the hydrolysis product, and this process is presented in Fig. 1. Low energy consumption and simultaneous recovery of the main byproduct were expected in the process. Static experiments were systematically carried out to obtain basic experimental data and explore the mechanism of adsorption. The breakthrough curve was investigated to analyze the dynamic kinetics. Optimization of operation conditions was carried out afterward.

## 2. Materials and methods

### 2.1. Chemicals and adsorbents

All the chemicals were of analytical grade from Kelong Chemical Reagent Factory, Chengdu, China.

Furfural was distilled under vacuum prior to its use. The macroporous resins D101, D141, and D100 were obtained from Blue-star Chengrand Chemical Co. Ltd, Chengdu, China. D301 anion exchange resin, 732 type cation exchange resin, activated carbon, and polyamides were supplied by Maoye Chemical Co. Ltd, Chongqing, China. The characteristics of the adsorbents are presented in Table 1.

### 2.2. Analytical measurements

Furfural content was determined by a UV detector (Beijing Puxi General Instrument Co., Ltd, Beijing, China) at 276 nm, which is the wavelength corresponding to the maximum absorbance of furfural. The linear range in the calibration curve ( $y = 0.15833x + 0.00128$ , where  $y$  was the absorbance value of the sample and  $x$  was the sample concentration) was 0.7–7 mg/L ( $R^2 = 0.9997$ ). All the samples were diluted within the linear range before they were accurately determined for furfural concentration. The content of acetic acid was determined by titration with 1 mol/L sodium hydroxide aqueous solution. The variations in measurements which could be attributed to experimental error were estimated to be less than 3%.

### 2.3. Static adsorption and desorption tests

#### 2.3.1. Selection of adsorbents and desorption reagent

All the adsorbents were pre-treated in accordance with the handling instructions to remove the impurities. Certain adsorbents were placed in a series of conical flasks containing 50 mL of 1% (w/w) furfural solution. The conical flasks were then shaken at 180 rpm in a constant temperature shaker (Guosheng Experimental Instrument Factory, Jiangsu, China) for 10 h at 298 K; after full adsorption equilibrium, the residual furfural concentration was determined by a UV detector, and the adsorption capacity of each adsorbent was then calculated and compared as follows:

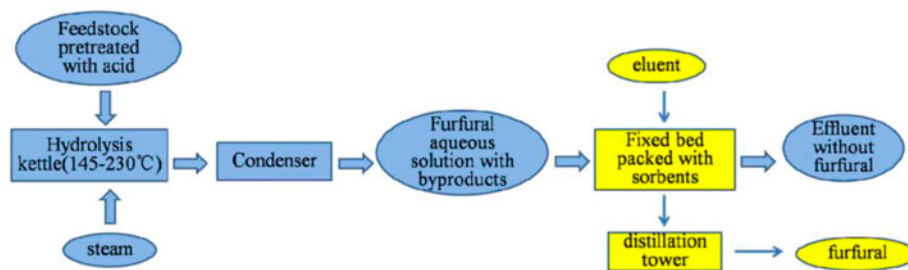


Fig. 1. The adsorption process of furfural.

Table 1  
Physical and chemical characteristics of the tested adsorbents

	Surface area (m <sup>2</sup> /g)	Pore diameter (Å)	Bulk capacity (g/mL)	Particle size (mm)	Polarity adsorption
D101 macroporous resin	500–550	90–100	0.65–0.7	0.3–1.25	Nonpolar
D141 macroporous resin	500–600	80	0.7	0.3–1.0	Nonpolar
D100 macroporous resin	500–600	75	0.7	0.3–1.0	Weak polar
732 type cation exchange resin	11.2	None	0.75–0.85	0.3–1.2	Strong polar
Activated carbon	850	200–15,000	0.45–0.55	0.074–0.15	Nonpolar
Polyamides	5–10	4,500–10,000	0.25	0.074–0.15	Polar
D301 anion exchange resin	30–40	45	0.65–0.72	0.315–1.25	Strong polar

$$q = (C_0 - C_e) \times V/m \quad (1)$$

where  $q$  (mg/g) is the adsorption capacity,  $C_0$  (mg/mL) is the initial concentration,  $C_e$  (mg/mL) is the equilibrium concentration,  $V$  (mL) is the solution volume, and  $m$  (g) is the dried mass of adsorbents. As macroporous resins were used in aquiferous state, the dried mass was converted by its moisture content. In this paper, all the adsorption capacities were calculated in this way unless specified.

Adsorbents with good adsorption behavior were selected, and solvent desorption behavior was then investigated with 50 mL of ethanol and butyl acetate as desorption reagents, respectively.

### 2.3.2. Adsorption selectivity of furfural with acetic acid and effect of pH on adsorption

As in earlier reported literature [2,19], furfural solution in practical production processes contained furfural, acetic acid, and traces of other low-boiling impurities. Adsorption selectivity of furfural with acetic acid and pH value of the solution were important factors for adsorption. Solutions containing furfural and acetic acid were prepared in accordance with the literature [19,20], including solution A (1% furfural, 0.25% acetic acid), solution B (5% furfural, 1.25% acetic acid), and solution C (8.3% furfural, 2% acetic acid); pH was adjusted with solid Na<sub>2</sub>CO<sub>3</sub> when required (for solution A, the pH was adjusted to 2.7, 4.0, 5.0, 6.0, and 7.1, respectively; for solution B, the pH was adjusted to 2.4, 3.0, 4.0, 5.1, 6.0, and 7.1, respectively; and for solution C, the pH was adjusted to 2.3, 3.0, 4.0, 5.0, 6.2, and 7.2, respectively). After static adsorption, the contents of furfural and acetic acid in the solution were determined. The adsorbents were then filtered and immersed in the desorption reagents to desorb furfural, and the content of furfural in the desorption solution was also determined. Blank runs, without adding adsorbent dose as control, were

performed simultaneously under the same conditions to eliminate experimental error from the degradation of furfural.

### 2.3.3. Adsorption kinetics and isotherms on resin

Five 50 mL aliquots of the sample solutions (obtained as described in Section 2.3.2) were placed in individual conical flasks containing certain D141 resins. The conical flasks were then shaken at 180 rpm in a constant temperature shaker; the furfural content at intervals from 30 s to 11 min was determined and the kinetic curves were then obtained. Also, the blank aqueous solution of furfural without adding adsorbent dose was agitated to check the stability of furfural during a time period of 1 h. It was found that furfural was stable in the solution and no change in concentration was observed during the time.

The adsorption isotherms of furfural on the sorbent were studied at different temperatures. Thus, eight 50 mL aliquots of sample solutions with different initial concentrations were placed in individual conical flasks containing 7 g hydrated resins. The conical flasks were then shaken at 180 rpm for 2 h to reach equilibrium at temperatures of 283, 293, 303, and 313 K, respectively. The degree of correlation between the adsorption data was thereby obtained, and relative Freundlich and Langmuir equations were evaluated.

### 2.4. Dynamic adsorption tests

Dynamic adsorption experiments were carried out on fixed bed (20.36 mm i.d., 500 mm height) wet-packed with resin. The bed volume (BV) of the resin was 45.7 mL, while the packed length of the resin bed was 150 mm. The sample solution (5% furfural) was pumped into the column at a flow rate of 3 mL/min, and the furfural content in the effluents was monitored by a UV detector. The relationship between  $C/C_0$  and time could be represented with a

breakthrough curve, where  $C$  represented the output concentration and  $C_0$  the feed adsorbate concentration. Significant parameters such as the mass transfer zone can be reflected in breakthrough curves, which played key roles in the design and operation of the fixed-bed adsorption process.

Orthogonal experimental design is widely used in the optimization of operation conditions, and in this work, factors, such as loading volume, loading velocity, elute volume, and elute velocity were selected as key parameters to optimize.

### 2.5. Isotherm models

The Langmuir adsorption isotherm expression is shown in Eq. (2) [21], and the model assumed that adsorption was monolayer. This was based on the assumption that the adsorbent surface consists of active sites having uniform energy, and therefore, the adsorption energy was constant [22].

$$\frac{C_e}{q_e} = \frac{1}{q_m K_L} + \frac{1}{q_m} C_e \quad (2)$$

where  $q_m$  (mg/g) is the maximum adsorption capacity,  $K_L$  (mL/mg) is the Langmuir constant,  $C_e$  (mg/mL) is the equilibrium concentration of solute in the solution, and  $q_e$  (mg/g) is the adsorption capacity at adsorption equilibrium.

In contrast, the Freundlich model was based on multilayer adsorption on the heterogeneous surface. It is assumed that the stronger binding sites were occupied first and that the binding strength decreased with increasing degree of site occupation. The Freundlich adsorption isotherm expression is shown in Eq. (3) [21].

$$\ln q_e = \ln K_F + \frac{1}{n} \ln C_e \quad (3)$$

where  $K_F$  is the parameter indicating adsorption capacity and  $1/n$  is an empirical parameter related to adsorption intensity.

### 2.6. Estimation of thermodynamic parameters

When furfural was adsorbed on the adsorbents and the residual furfural in the liquid phase remained constant, adsorption equilibrium was reached. Thermodynamic parameters such as Gibbs free energy change ( $\Delta G$ ), enthalpy change ( $\Delta H$ ), and entropy change ( $\Delta S$ ) were estimated from the following equations [23]:

$$K_D = \frac{q_e}{C_e} \quad (4)$$

$$\Delta G = -RT \ln K_D \quad (5)$$

$$\Delta G = \Delta H - T\Delta S \quad (6)$$

$$\ln K_D = \frac{\Delta S}{R} - \frac{\Delta H}{RT} \quad (7)$$

where  $K_D$  is the distribution coefficient (mL/g), and  $R$  is the gas constant (8.314 J/(mol K)). The thermodynamic parameters of  $\Delta H$  and  $\Delta S$  can be obtained from the slope and intercept of the Van't Hoff plot of  $\ln K_D$  vs.  $1/T$ . Then, Eq. (6) was applied to calculate the standard Gibbs free energy.

### 2.7. Adsorption kinetic study

Both pseudo-first- and second-order adsorption models were used to describe the adsorption kinetics data [24]. In both models, all the steps of adsorption, such as external diffusion, internal diffusion, and adsorption were lumped together, and it was assumed that the difference between the average solid phase concentration and the equilibrium concentration was the driving force for adsorption, and that the overall adsorption rate was proportional to either the driving force (as in the pseudo-first-order equation) or the square of the driving force (as in the pseudo-second-order equation) [25].

$$\text{Pseudo-first-order model : } \ln(q_e - q) = \ln q_e - kt \quad (8)$$

$$\text{Pseudo-second-order model : } \frac{t}{q} = \frac{1}{kq_e^2} + \frac{t}{q_e} \quad (9)$$

where  $q_e$  (mg/g) is the adsorption capacity at adsorption equilibrium,  $q$  (mg/g) is the adsorption capacity at time  $t$ , and  $k$  is the rate constant.

## 3. Results and discussion

### 3.1. Selection of adsorbents

Seven kinds of adsorbents mentioned in Section 2.1 were used to adsorb furfural, and the adsorption capacities are shown in Fig. 2. Among them, activated carbon and some macroporous resins obtained better adsorption efficacy than the exchange resins and polyamides. The separation mechanism of exchange resins (732 type and D301) was ionic exchange, while for polyamides, hydrogen bonds drove separation.

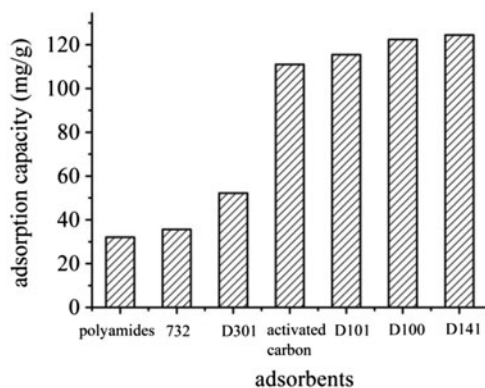


Fig. 2. Comparison of adsorption capacity of seven kinds of adsorbents.

The result implied that the adsorption of furfural was dominated by the van der Waals force between adsorbents and furfural, which was highly relative to the surface area. Besides, the pore diameter and the polarity of the sorbents were also important factors for the adsorption of furfural. For the systemic investigation of these factors, further experiments using more kinds of adsorbents with various parameters are needed. D141 and D100 macroporous resins were chosen because of their high adsorption capacities, and activated carbon was also selected in the desorption study for lower cost and wide application.

In our study, ethanol and butyl acetate were used to desorb furfural, and their desorption ratios are shown in Fig. 3. Actually, the desorption could be regarded as the distribution of furfural on the surface of solid phase and the desorption reagent. The result showed that the desorption ability of butyl acetate was slightly higher than that of ethanol. It could be explained by the similar polarity of furfural and butyl

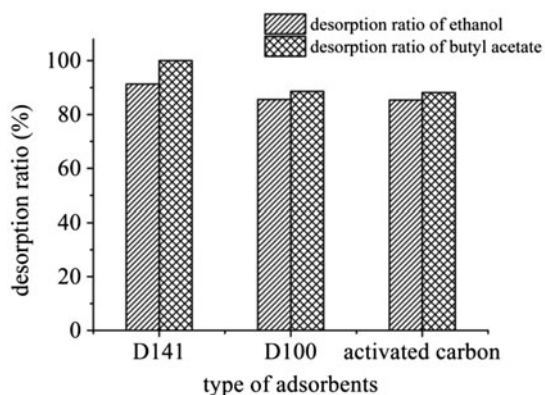


Fig. 3. Comparison of desorption ratio of three adsorbents.

acetate. Besides, the resin was non-polar or weak polar, and its affinity to butyl acetate was stronger than ethanol. However, a 100% desorption rate could not be achieved even for butyl acetate. The explanation was that a certain adsorption capacity of furfural on adsorbents existed in organic solution just as in aqueous solution, which varied with adsorbents and organic reagents.

As the latent heat of vaporization of ethanol (38.95 kJ/mol) is much lower than that of butyl acetate (309.3 kJ/mol), which indicated low energy consumption in the distillation stage, ethanol was chosen as the desorption reagent. Based on the comparison of the adsorption and desorption ratios of each sorbent, it was found that D141 had perfect capacity. So it was selected in further studies.

### 3.2. Adsorption selectivity of furfural with acetic acid and effect of pH on adsorption

#### 3.2.1. Adsorption selectivity of furfural and acetic acid

As acetic acid is the main byproduct of furfural production, adsorption selectivity was observed. As shown in Fig. 4, the adsorption ratio of furfural was much higher than that of acetic acid, but the separation was far away from 100%, for some of the acetic acid was also adsorbed. The result suggested that in a dynamic adsorption process, furfural could be adsorbed while most acetic acid remains in the effluent, i.e. perfect selectivity has not been achieved by the D141 resin, and thus, adsorbents with higher selectivity of furfural to acetic acid need to be developed.

#### 3.2.2. Effect of pH value and electrolyte

Another recovery form of acetic acid is sodium acetate, which is simple and commonly used in

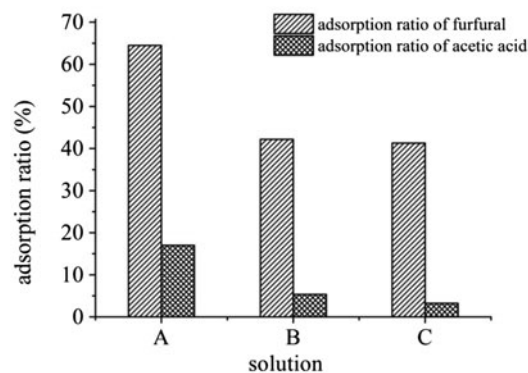


Fig. 4. Adsorption selectivity of furfural and acetic acid.

conventional processes. Once  $\text{Na}_2\text{CO}_3$  was added in the sample solutions, the constituents became complex with the existence of acetic acid, furfural, and sodium acetate. The effects of pH and electrolyte on furfural adsorption have been separately evaluated in literature [16]. However, the integrated influence of both pH and electrolyte has not been investigated. So, in this work, the analysis of their different influences on adsorption and desorption from sample to sample are shown in Fig. 5. For solution A, the adsorption and desorption ratios tended to be at a constant level without obvious change, since the content of acetic acid and sodium acetate was much less than in solutions B and C. For solution B, the adsorption ratio was highest at pH 5.16, which was caused by the presence of electrolyte. For solution C, the adsorption ratio increased with higher pH, which should result from the salting-out effect. Initial solution C was saturated with furfural, and inorganic salt was generated in the process of adjusting pH by  $\text{Na}_2\text{CO}_3$ , leading to the decrease of furfural solubility in water. The concentrations of furfural in aqueous phase under different pH are shown in Fig. 6.

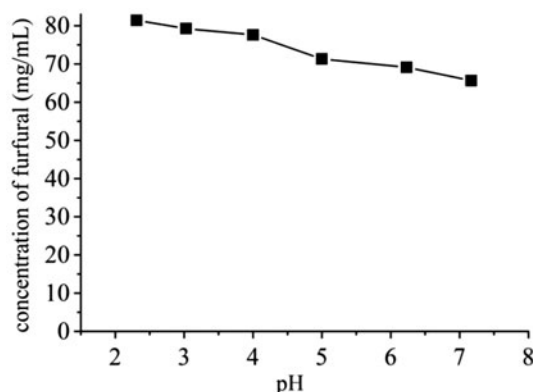


Fig. 6. Effect of pH and electrolyte on the solubility of furfural.

On the other hand, the desorption ratios of solutions B and C tended to have two peaks at the working pH range. It suggested that moderate acetic acid and sodium acetate were good for desorption. In general, as acetic acid was converted into sodium acetate at around pH 6, the adsorption and desorption

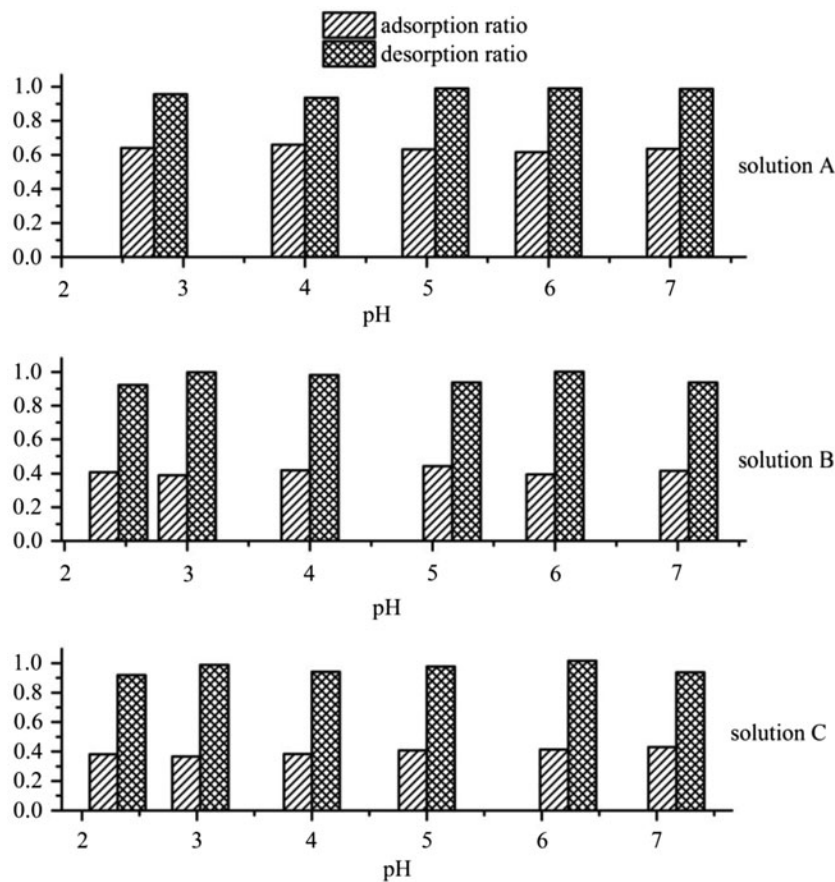


Fig. 5. Effect of pH and electrolyte on the adsorption and desorption ratios.

ratios were satisfied and the recovery of sodium acetate in the effluent was feasible.

### 3.3. Adsorption kinetics onto D141 resin

The concentration of furfural in the liquid phase was determined at different time intervals until equilibrium was reached, and the corresponding results are depicted in Fig. 7. It can be seen that the adsorption capacity increased with longer adsorption time. Thus, the adsorption amount increased rapidly during the first 5 min, followed by a declined rate, and then it took 10 min to reach equilibrium. In the reported literature, the equilibrium time for the adsorption of furfural was relatively longer (1 h for MCM-48-AS [17], and 6 h for activated carbon [18]) with low concentration (0.05–1 mg/mL) of furfural in the initial solution. Hence, the D141 resin only needed a very short contact time to reach equilibrium with furfural. This result proved that the concentration of adsorbent should be the dominant driven force for furfural adsorption.

The experimental data of furfural adsorption were fitted with pseudo-first-order (Eq. (8)) and pseudo-second-order (Eq. (9)) models. The rate constants and coefficient of determination ( $R^2$ ) values are summarized in Table 2.  $q_{e,exp}$  and the  $q_{e,cal}$  values from the pseudo-second-order kinetic model were very close to each other. The squares of correlation coefficients are also closer to unity for the pseudo-second-order kinetic model than the pseudo-first-order kinetic model. Therefore, the adsorption can be approximated more precisely by the pseudo-second-order kinetic model. Compared with the adsorption rate constant, it was estimated that the duration for equilibrium increased with the concentration, and also could be affected by pH and electrolyte.

### 3.4. Adsorption isotherms on D141 resin

Fig. 8 showed the furfural adsorption capacity,  $q_e$  (mg/g), onto D141 versus the equilibrium concentration  $C_e$  (mg/mL) under various temperatures (283, 293, 303, and 313 K, respectively). The shapes of

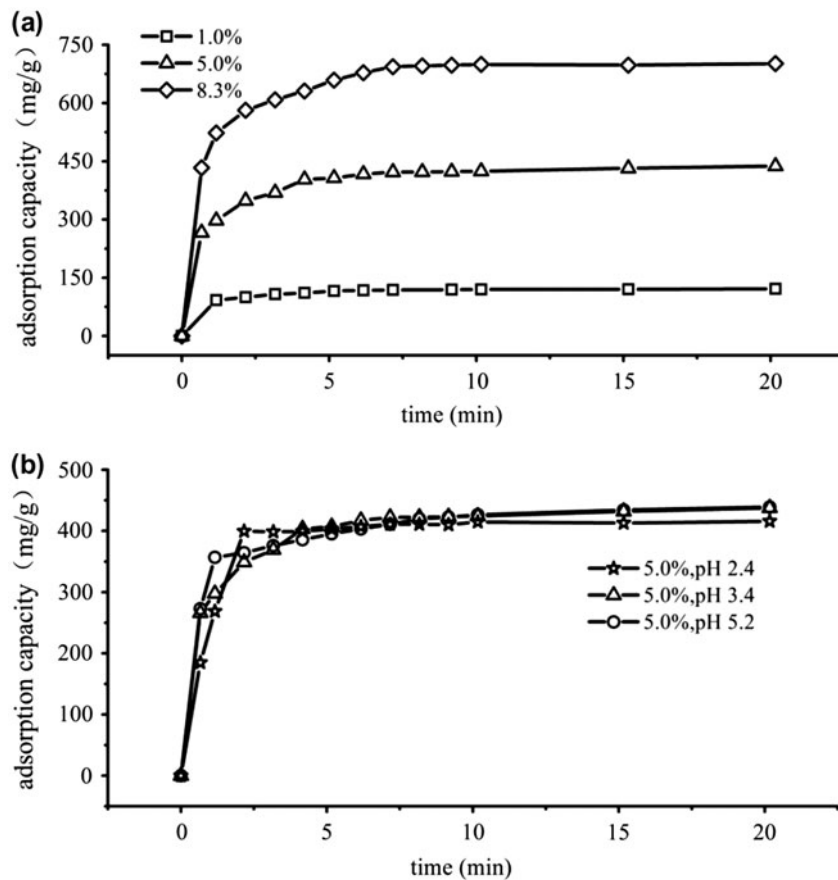


Fig. 7. Adsorption kinetics curves (298 K) ((a) effect of furfural concentration; (b) effect of pH and electrolyte).

Table 2  
Pseudo-first-order and pseudo-second-order model constants

Samples	Pseudo-first-order				Pseudo-second-order			
	$q_{e,exp}$	$q_{e,cal}$	$k$	$R^2$	$q_{e,exp}$	$q_{e,cal}$	$k$	$R^2$
1%	121.3	117.2	1.12	0.9839	121.3	124.0	0.0192	0.9998
5%	437.6	415.7	1.17	0.9702	437.6	449.1	0.00409	0.9998
8.3%	701.5	675.0	1.30	0.9726	701.5	721.5	0.00312	0.9996
5%, pH 2.44	415.8	413.0	0.98	0.9908	415.8	426.8	0.00593	0.9987
5%, pH 5.16	439.1	409.7	1.59	0.9703	439.1	449.1	0.00398	0.9995

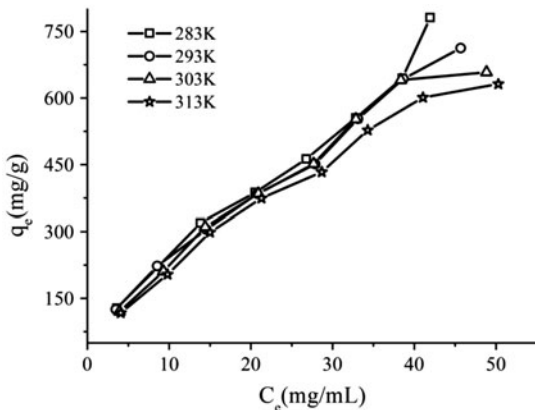


Fig. 8. Adsorption isotherms.

the isotherms were different from the adsorbents in Jeřábek's research [8]. However, when  $C_e$  was about 4%, the  $q_e$  of D141 was similar with that of Amberlite XAD-4 (about 550 mg/g), which had maximum adsorption capacity among the adsorbents studied. The Langmuir parameters ( $K_L$  and  $q_m$ ) and Freundlich parameters ( $K_F$  and  $n$ ) for the adsorption isotherms are given in Table 3. According to the square of correlation coefficient ( $R^2$ ), the Freundlich isotherm was more suitable to describe the adsorption equilibrium of furfural onto D141. Values of  $n$  higher than 1 revealed the favorable adsorption of furfural onto

D141. In contrast to the adsorption isotherms of furfural onto as-synthesized MCM-41 and MCM-48 [16], whose  $q_m$  was 188.6 and 196.1 mg/g, respectively, it can be found that the D141 macroporous resin was more favorable for adsorption of furfural at high concentration.

### 3.5. Adsorption thermodynamics on D141

$\Delta H$  (enthalpy change) and  $\Delta S$  (entropy change) were obtained as two key thermodynamic parameters from the slope and intercept of the Van't Hoff plot of  $\ln K_D$  vs.  $1/T$  (Fig. 9). Then, Eq. (6) was applied to calculate the standard Gibbs free energy (see Table 4). The negative  $\Delta G$  indicated that the adsorption of furfural on D141 was spontaneous for the investigated temperature range, which was usually the case for many common adsorption systems in solution. The negative  $\Delta H$  showed that the adsorption was exothermic [26], so the increasing temperature leads to lower adsorption of furfural at equilibrium. The values of adsorption heat which were less than 40 kJ/mol indicated physical adsorption mechanism. Positive  $\Delta S$  indicated a decrease in the order of the system.

### 3.6. Breakthrough curve on D141 resin

The breakthrough curve of adsorption is shown in Fig. 10. Through the steep slope of the breakthrough

Table 3  
Isotherm parameters for furfural adsorption on D141

Temperature (K)	Langmuir isotherm			Freundlich isotherm		
	$K_L$ (mL/mg)	$Q_m$ (mg/g)	$R^2$	$K_F$	$n$	$R^2$
283	0.02154	1,415	0.768	36.8718	1.2608	0.972
293	0.02455	1,252	0.846	42.8114	1.3658	0.989
303	0.02325	1,249	0.919	49.0970	1.4662	0.981
313	0.02612	1,104	0.933	52.4494	1.5524	0.983

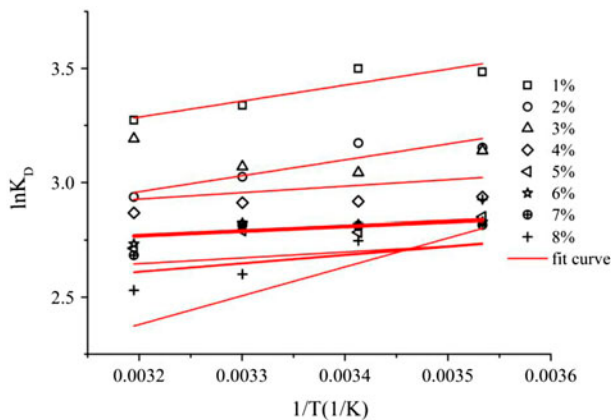


Fig. 9. Van't Hoff plots for furfural adsorption onto D141 at different initial furfural concentrations.

curve, the rate of mass transfer was found to be very rapid, which was further confirmed in the static kinetics study (Section 3.3). It was found that the value of  $t_b$  (time taken for breakthrough, when the outlet concentration approached 5% of the initial feed concentration) was 48 min. At this point, the adsorption capacity was calculated to be 628 mg/g (dried resin).

### 3.7. Optimization of dynamic operation conditions

The orthogonal experimental results are displayed in Table 5. The recovery of furfural was calculated with Eq. (10):

$$Y = \frac{(C_2 \times V_2)}{(C_0 \times V_1)} \times 100\% \quad (10)$$

where  $Y$  (%) is the recovery of furfural,  $C_0$  (mg/mL) is the furfural concentration of the loading solution,  $V_1$  (mL) is the loading volume,  $C_2$  (mL) is the furfural

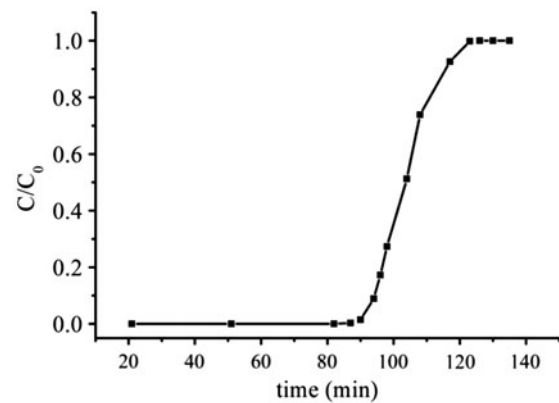


Fig. 10. Breakthrough curve for furfural adsorption onto D141.

concentration of the elute solution, and  $V_2$  is the elute volume. From the range of each factor, it could be found that the effects of loading velocity, loading volume, elution velocity, and elution volume decreased. Thus, the optimized process of adsorption was a 3 BV solution (1 BV = 10 mL resins in this experiment) loaded on the fixed bed with a velocity of 1 BV/h, then eluted by 1 BV ethanol with a velocity of 1 BV/h, and the optimal recovery of furfural was 96.97%. Through the adsorption process, the concentration of the loading solution improved two times in the ethanol solution; the elute with furfural could then be steamed to recover furfural with ethanol recycled. Significant decrease in energy consumption could be achieved in the distillation process when compared with the conventional process. As shown in Fig. 11, the reusability of D141 was perfect because little change had occurred when it was reused three times. However, the actual system for the adsorption process will be significantly different from the experimental result, and more practical factors should be taken into account in the actual system for adsorption.

Table 4  
Thermodynamic parameters for furfural adsorption on D141

Initial concentration (%)	$\Delta H$ (kJ/mol)	$\Delta S$ (J/mol K)	$\Delta G$ (kJ/mol)			
			283 (K)	293 (K)	303 (K)	313 (K)
1	-5.64	9.97	-8.46	-8.56	-8.66	-8.76
2	-5.56	7.63	-7.72	-7.79	-7.87	-7.95
3	-2.84	13.5	-6.68	-6.82	-6.95	-7.09
4	-1.57	18.8	-6.91	-7.10	-7.29	-7.48
5	-2.90	13.3	-6.69	-6.83	-6.96	-7.01
6	-1.99	16.5	-6.68	-6.85	-7.016	-7.18
7	-2.84	13.5	-6.68	-6.82	-6.95	-7.09
8	-9.84	-10.6	-6.83	-6.73	-6.62	-6.51

Table 5  
Orthogonal experimental design and results

Number	Loading volume (BV)	Loading velocity (BV/h)	Elution velocity (BV/h)	Elution volume (BV)	Recovery of furfural (%)
1	3	1	1	1	96.9
2	3	3	3	3	84.2
3	3	5	5	5	91.7
4	4	1	3	5	92.2
5	4	3	5	1	78.0
6	4	5	1	3	90.3
7	5	1	5	3	86.7
8	5	3	1	5	81.6
9	5	5	3	1	72.7
Mean value 1	90.99	91.98	89.653	82.577	
Mean value 2	86.87	81.293	83.077	87.144	
Mean value 3	80.370	84.957	85.5	88.513	
Range	10.620	10.687	6.576	5.936	

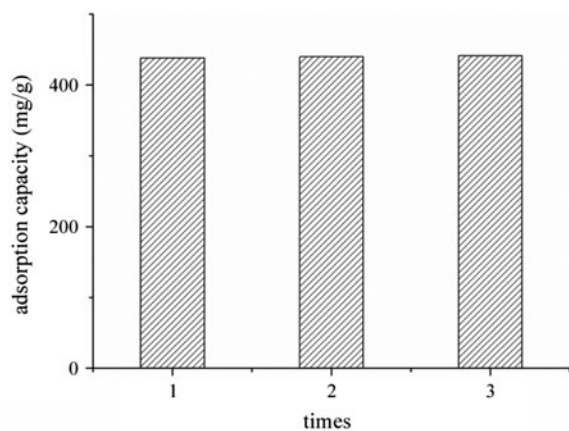


Fig. 11. The variance of the adsorption capacity of furfural during the course of continuous use of D141 macroporous adsorption resin.

#### 4. Conclusion

In this work, the adsorption characteristics of furfural on macroporous resin were systematically studied and an effective procedure was established. D141 macroporous resin showed good adsorption performance, which was more favorable for the adsorption of furfural at high concentrations than currently reported adsorbents. Ethanol was found to be an ideal desorption reagent for its low latent heat of vaporization. Adsorption kinetics revealed that the adsorption rate was rapid and fitted for pseudo-second-order model. The Freundlich isotherm was more suitable to describe the adsorption equilibrium of furfural onto D141. The values of  $n$  which were higher than 1 revealed favorable adsorption of furfural onto D141.

Adsorption thermodynamic parameters demonstrated that the adsorption was a spontaneous, exothermic, physical, and entropy-increased process. The value of pH and electrolyte had no significant effect on the adsorption of furfural; however, the adsorption selectivity of furfural and acetic acid has shown the potential to be further explored to recover furfural and acetic acid simultaneously, which will be discussed in the future. Under optimized adsorption and desorption conditions, the multiple of concentration for a 5% furfural aqueous solution was about 3, which indicated that energy consumption was reduced to a certain extent. Nonetheless, the adsorption capacity should be improved to achieve a higher multiple of concentration for the diluted furfural aqueous solution.

#### References

- [1] A.S. Mamman, J.M. Lee, Y.C. Kim, I.T. Hwang, N.J. Park, Y.K. Hwang, J.S. Chang, J.S. Hwang, Furfural: Hemicellulose/xylose derived biochemical, *Biofuels, Bioprod. Biorefin.* 2 (2008) 438–454.
- [2] J.P. Lange, E. van der Heide, J. van Buijtenen, R. Price, Furfural—A promising platform for lignocellulosic biofuels, *ChemSusChem* 5 (2012) 150–166.
- [3] K.J. Zeitsch, *The Chemistry and Technology of Furfural and its Many By-Products*, Sugar series, Elsevier, Amsterdam, 2000.
- [4] B.F. De Almeida, T.M. Waldrigui, T.D. Alves, L.H. De Oliveira, M. Aznar, Experimental and calculated liquid–liquid equilibrium data for water + furfural + solvents, *Fluid Phase Equilib.* 334 (2012) 97–105.
- [5] A.C.G. Marigliano, M.B.G. De Doz, H.N. Sólamo, Influence of temperature on the liquid–liquid equilibria containing two pairs of partially miscible liquids: water + furfural + 1-butanol ternary system, *Fluid Phase Equilib.* 153 (1998) 279–292.

- [6] S. Moulik, P. Khandelwal, Recovery of furfural from the prehydrolysis vapor vent condensate from a dissolving pulp plant, *Res. Ind.* 34 (1989) 205–210.
- [7] T. Sako, T. Sugeta, N. Nakazawa, K. Otake, M. Sato, K. Ishihara, M. Kato, High pressure vapor–liquid and vapor–liquid–liquid equilibria for systems containing supercritical carbon dioxide, water and furfural, *Fluid Phase Equilib.* 108 (1995) 293–303.
- [8] K. Jeřábek, L. Hankova, Z. Prokop, Post-crosslinked polymer adsorbents and their properties for separation of furfural from aqueous solutions, *React. Polym.* 23 (1994) 107–112.
- [9] U.K. Ghosh, N.C. Pradhan, B. Adhikari, Pervaporative separation of furfural from aqueous solution using modified polyurethaneurea membrane, *Desalination* 252 (2010) 1–7.
- [10] X.L. Liu, H. Jin, Y.S. Li, H. Bux, Z.Y. Hu, Y.J. Ban, W.S. Yang, Metal–organic framework ZIF-8 nanocomposite membrane for efficient recovery of furfural via pervaporation and vapor permeation, *J. Membr. Sci.* 428 (2013) 498–506.
- [11] E.I. Gürbüz, S.G. Wettstein, J.A. Dumesic, Conversion of hemicellulose to furfural and levulinic acid using biphasic reactors with alkylphenol solvents, *ChemSusChem* 5 (2012) 383–387.
- [12] C. Rong, X. Ding, Y. Zhu, Y. Li, L. Wang, Y. Qu, X. Ma, Z. Wang, Production of furfural from xylose at atmospheric pressure by dilute sulfuric acid and inorganic salts, *Carbohydr. Res.* 350 (2012) 77–80.
- [13] I. Agirrezabal-Telleria, A. Larreategui, J. Requies, M.B. Güemez, P.L. Arias, Furfural production from xylose using sulfonic ion-exchange resins (Amberlyst) and simultaneous stripping with nitrogen, *Bioresour. Technol.* 102 (2011) 7478–7485.
- [14] S. Lucas, M.J. Cocero, C. Zetzl, G. Brunner, Adsorption isotherms for ethylacetate and furfural on activated carbon from supercritical carbon dioxide, *Fluid Phase Equilib.* 219 (2004) 171–179.
- [15] P. Gupta, A. Nanoti, M. Garg, A. Goswami, The removal of furfural from water by adsorption with polymeric resins, *Sep. Sci. Technol.* 36 (2001) 2835–2844.
- [16] M. Anbia, N. Mohammadi, K. Mohammadi, Fast and efficient mesoporous adsorbents for the separation of toxic compounds from aqueous media, *J. Hazard. Mater.* 176 (2010) 965–972.
- [17] M. Anbia, N. Mohammadi, A nanoporous adsorbent for removal of furfural from aqueous solutions, *Desalination* 249 (2009) 150–153.
- [18] A.K. Sahu, V.C. Srivastava, I.D. Mall, D.H. Lataye, Adsorption of furfural from aqueous solution onto activated carbon: Kinetic, equilibrium and thermodynamic study, *Sep. Sci. Technol.* 43 (2008) 1239–1259.
- [19] L. Yao-Jun, On the pollution from producing furfural with corncob [J], *J. Luohe Vocational Technol. College* 2 (2009) 9–11.
- [20] L. Zhaolin, S. Yuqing, Y. Dan, C. Fengjun, Z. Hua, Industrial design and simulation on extraction process of furfural as  $\text{CHCl}_3$  extraction, *Guangdong Chem. Ind.* 38 (2011) 109–110.
- [21] Z. Chowdhury, S. Zain, A. Rashid, Equilibrium isotherm modeling, kinetics and thermodynamics study for removal of lead from waste water, *J. Chem.* 8 (2011) 333–339.
- [22] T.S. Anirudhan, P. Senan, Adsorption characteristics of cytochrome C onto cationic Langmuir monolayers of sulfonated poly(glycidylmethacrylate)-grafted cellulose: Mass transfer analysis, isotherm modeling and thermodynamics, *Chem. Eng. J.* 168 (2011) 678–690.
- [23] Q. Li, L. Chai, Z. Yang, Q. Wang, Kinetics and thermodynamics of Pb(II) adsorption onto modified spent grain from aqueous solutions, *Appl. Surf. Sci.* 255 (2009) 4298–4303.
- [24] K. Tong, M.J. Kassim, A. Azraa, Adsorption of copper ion from its aqueous solution by a novel biosorbent *Uncaria gambir*: Equilibrium, kinetics, and thermodynamic studies, *Chem. Eng. J.* 170 (2011) 145–153.
- [25] Z. Wu, H. Joo, K. Lee, Kinetics and thermodynamics of the organic dye adsorption on the mesoporous hybrid xerogel, *Chem. Eng. J.* 112 (2005) 227–236.
- [26] L. You, Z. Wu, T. Kim, K. Lee, Kinetics and thermodynamics of bromophenol blue adsorption by a mesoporous hybrid gel derived from tetraethoxysilane and bis(trimethoxysilyl)hexane, *J. Colloid Interface Sci.* 300 (2006) 526–535.